

Characteristic Raindrop Size Retrievals from Measurements of Differences in Vertical Doppler Velocities at Ka- and W-Band Radar Frequencies

SERGEY Y. MATROSOV

Cooperative Institute for Research in Environmental Sciences, University of Colorado Boulder, and NOAA/Earth System Research Laboratory, Boulder, Colorado

(Manuscript received 21 September 2016, in final form 4 October 2016)

ABSTRACT

A Ka-band (~35 GHz) and W-band (~94 GHz) radar approach to retrieve profiles of characteristic raindrop sizes, such as mean mass-weighted drop diameters D_m , from measurements of the difference in the mean vertical Doppler velocities (DDV) is analyzed. This retrieval approach is insensitive to radar calibration errors, vertical air motions, and attenuation effects. The D_m -DDV relations are derived using long-term measurements of drop size distributions (DSDs) from different observational sites and do not assume a functional DSD shape. Unambiguous retrievals using this approach are shown to be available in the D_m range of approximately 0.5–2 mm, with average uncertainties of around 21%. Potential retrieval ambiguities occurring when larger drop populations exist can be avoided by using a Ka-band vertical Doppler velocity threshold. The performance of the retrievals is illustrated using a long predominantly stratiform rain event observed at the Atmospheric Radiation Measurement (ARM) Southern Great Plains site. An intercomparison of DDV-based estimates of characteristic raindrop sizes with independent estimates available from ground-based disdrometer measurements reveal good agreement, with a correlation coefficient of 0.88, and mean differences between radar and disdrometer-based D_m of approximately 14% for the entire range of unambiguous retrievals. The Ka–W-band DDV method to retrieve mean mass-weighted drop sizes is applicable to measurements from new dual-wavelength ARM cloud radars that are being deployed at a variety of observational facilities. An illustration for the retrievals at the Orlitok Point ARM facility is also given.

1. Introduction

The variability of hydrometeor microphysical parameters (e.g., raindrop characteristic size) influences vertical profiles of radar measurements and is therefore important for quantitative precipitation estimations using weather radars. Information on the vertical profiles of drop size distribution (DSD) parameters is also crucial for understanding rainfall processes, including drop breakup, collision–coalescence, and evaporation.

If the differential attenuation is known, Doppler spectra from vertically pointing measurements at two cloud radar frequencies can be used to retrieve binned DSD information when mean volume drop diameters are greater than about 1 mm and air spectral broadening is small (e.g., [Tridon and Battaglia 2015](#)). Dual-frequency Doppler moment measurements from vertically pointing

radars have also been used to infer individual rain DSD parameters (e.g., [Tian et al. 2007](#); [Liao et al. 2008](#); [Williams et al. 2016](#)). If hydrometeor scattering is at least one frequency outside the Rayleigh regime, the difference in radar moments (e.g., equivalent reflectivity factors, Doppler velocities) at these frequencies depends on the DSD parameters. Unlike the reflectivity factor ratios, differences between mean vertical Doppler velocities (DDV) are immune to differential attenuation and absolute radar calibration uncertainties. Moreover, DDV measurements are less susceptible to spectral broadening (compared to Doppler spectra measurements) and they are immune to vertical air motions, which hamper the use of single-frequency vertically pointing Doppler radar-based retrievals of DSD parameters.

DDV measurements can be used to estimate the median volume drop size D_o or the mean mass-weighted drop size D_m . Here, nonspherical raindrop sizes are understood as diameters of equal-volume spheres. Traditionally, relations between the characteristic drop size and DDV, as used for subsequent retrievals, are modeled assuming a three-parameter gamma-function DSD

Corresponding author address: Sergey Y. Matrosov, NOAA/ESRL/Physical Sciences Division, R/PSD2, 325 Broadway, Boulder, CO 80305.

E-mail: sergey.matrosov@noaa.gov

shape. Different combinations of radar frequencies, ν_1 and ν_2 , have been used to derive characteristic raindrop size information from DDV measurements assuming a gamma-function DSD type. For retrievals of D_o , which is one of the gamma-function parameters, Tian et al. (2007) and Liao et al. (2008) used airborne nadir-pointing X-band ($\nu \sim 10$ GHz) and W-band ($\nu \sim 94$ GHz) measurements, while Williams et al. (2016) used ground-based vertically pointing S-band ($\nu \sim 3$ GHz) and Ka-band ($\nu \sim 35$ GHz) measurements for D_m characteristic size estimates. Giangrande et al. (2012) used a Doppler spectra inversion technique applied to ground-based W-band spectral measurements to retrieve D_o . These authors also indicated a potential for Ka–W-band DDV-based estimates of D_o and related it to gamma-function DSD modeling results. The X–W-band and Ka–W-band DDV measurements were also used previously for inferring characteristic sizes of ice/snow particles (e.g., Liao et al. 2008; Matrosov 2011). Modeling with the gamma-function rain DSDs (Tian et al. 2007; Liao et al. 2008) indicated the occurrence of ambiguous correspondence between DDV and D_o , as very large values of D_o can result in DDV values similar to those produced by smaller drop populations. The objective of this study is to evaluate Ka–W-band vertical DDV measurements for retrieving characteristic raindrop sizes.

2. Relations between DDV and raindrop characteristic sizes

Recently, the adequacy of the gamma-function representation of rain DSDs has been questioned (e.g., Adirosi et al. 2015; Ekerete et al. 2015). Liao et al. Meneghini (2008) also pointed out that dual-wavelength approaches suffer from a possible inaccuracy of the gamma-function DSD assumption. To avoid inconsistencies in describing natural raindrop spectra, this study uses observed DSDs without fitting observations by a functional form. Impact Joss–Waldvogel disdrometers (JWD; Joss and Waldvogel 1967) and optical Particle Size and Velocity (Parsivel; Löffler-Mang and Joss 2000) disdrometers have been used to observe DSD properties. These instruments provide drop counts in a number of size

bins centered at particular diameters D_i (where i is the bin number), which are then used to calculate binned drop concentrations $n(D_i)$.

Mean mass-weighted drop sizes D_m are calculated from disdrometer data as

$$D_m = \frac{\sum_i D_i^4 n(D_i)}{\sum_i D_i^3 n(D_i)}, \quad (1)$$

where the summation is performed over all bin sizes. The median volume size D_o is usually very close to D_m . Note that for the gamma-function DSD $D_o \approx D_m (3.67 + \mu)/(4 + \mu)$, where μ is the gamma-function shape parameter (e.g., Brangi and Chandrasekar 2001). Hereinafter, D_m is used as a characteristic DSD size because it can be directly calculated from disdrometer data. Vertical Doppler velocities due to drop terminal fall speeds at a frequency ν are expressed as

$$V_{D\nu}(\nu) = \frac{\sum_i \sigma(D_i) n_i(D_i) V_t(D_i)}{\sum_i \sigma(D_i) n_i(D_i)}, \quad (2)$$

where σ are the backscatter cross sections and V_t are the drop fall speeds. In this study V_t values for normal atmospheric conditions were calculated using Wobus et al. (1971) data, and the σ values were computed using the T-matrix method assuming a nonspherical drop shape model from Brandes et al. (2005).

Figure 1a shows a scatterplot of Ka–W-band DDV [i.e., $\text{DDV} = V_D(35 \text{ GHz}) - V_D(94 \text{ GHz})$, which is the same as $\text{DDV} = V_{D\nu}(35 \text{ GHz}) - V_{D\nu}(94 \text{ GHz})$, since the observed Doppler velocities $V_D = V_{D\nu} + V_a$, where V_a is a vertical air motion] versus D_m as calculated using the JWD rain DSDs collected during a multimonth field project in California (Matrosov 2010). Figure 1b presents a Ka–W-band DDV– D_m scatterplot obtained from Parsivel DSD data observed during yearlong observations in the southeastern United States (Matrosov et al. 2016). For smaller drop populations ($D_m < 0.5$ mm), DDV is close to zero, since scattering is largely in the Rayleigh regime at both frequencies. Thus, there is practically no information in DDV measurements about D_m for such small drop populations. Mean Ka–W-band DDV– D_m relations from data in Figs. 1a and 1b can be approximated using the same piecewise power-law polynomial fit (blue lines in figures),

$$\begin{aligned} D_m(\text{mm}) &\approx 0.47 + 0.49 \text{DDV}^{0.54} \text{ (for } \text{DDV} \leq 1 \text{ m s}^{-1}\text{)}, \\ D_m(\text{mm}) &\approx 1.338 - 0.977 \text{DDV} + 0.678 \text{DDV}^2 - 0.079 \text{DDV}^3 \text{ (for } 1 \text{ m s}^{-1} < \text{DDV} < 2.4 \text{ m s}^{-1}\text{)}. \end{aligned} \quad (3)$$

From Figs. 1a and 1b it is apparent that in spite of the instrument differences and different locations of the

data collection sites, the scatterplots are quite similar even though the data scatter is somewhat larger for the

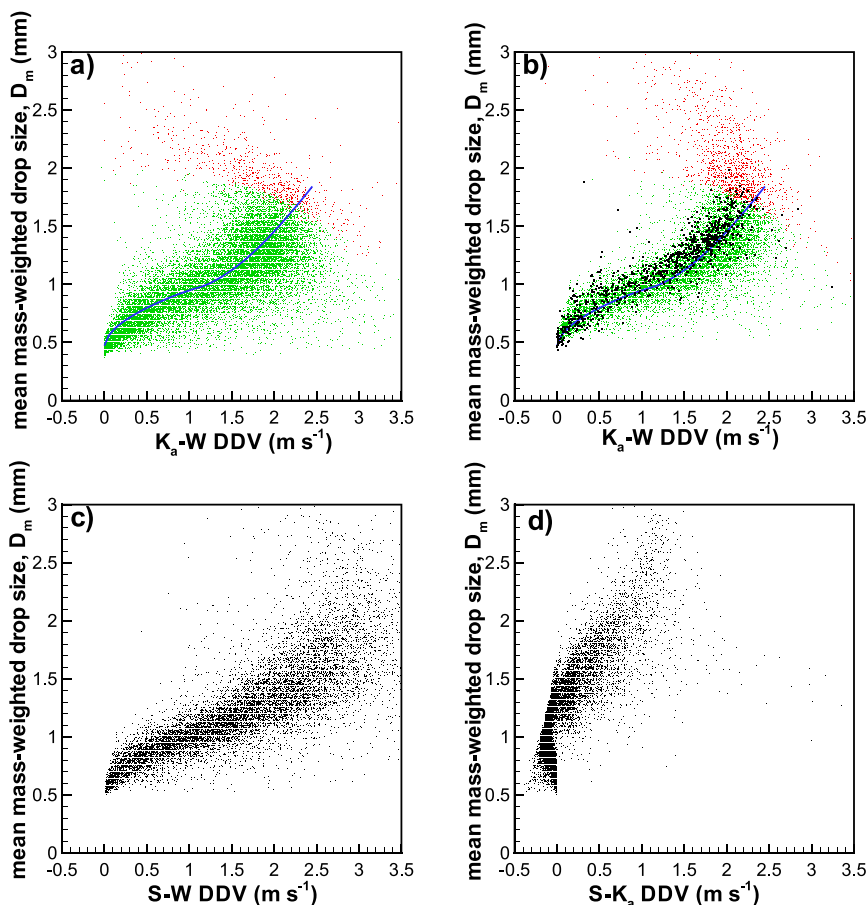


FIG. 1. Scatterplots of (a),(b) Ka–W-band DDV, (c) S–W-band DDV, and (d) S–Ka-band DDV vs D_m based on (a) Hydrometeorology Testbed (HMT) JWD and (b)–(d) HMT Parsivel observational DSDs for normal atmospheric conditions. Green (red) dots in (a) and (b) correspond to V_{Dr} (Ka band) smaller (larger) than 6.9 m s^{-1} . Black dots in (b) correspond to the SGP JWD data from 1 May 2007. The blue line in (a) and (b) corresponds to the fit given by Eqs. (3).

JWD dataset. Some distinctions exist in the region of smaller D_m values, which can be explained in part by disdrometer deficiencies in counting drops in smaller size bins. The “dead time” correction to alleviate the JWD undercount for smaller bin sizes (Sheppard and Joe 1994), however, was implemented in this study.

Except for a relatively small number of data points, the modeled Ka–W-band DDV values generally do not exceed 3 m s^{-1} . For higher DDV values, the DDV– D_m correspondence is not clearly defined, as both smaller and larger raindrop populations can produce similar Ka–W-band DDV values. This is better seen in the Parsivel data (Fig. 1b) because they were obtained during more frequent presence of heavier rainfall with larger D_m . For these larger drop populations, the general trend of the Ka–W-band DDV is not very distinct and there is a weak tendency of DDV decreasing as D_m increases beyond 2 mm or so.

The DDV-based D_m retrieval ambiguity, however, can be alleviated if heavier rainfall with larger drops is identified. One way to identify the larger D_m rainfall is to use an absolute V_D (35 GHz) threshold of about 6.9 m s^{-1} (red points in Figs. 1a and 1b). Exclusion of these data effectively eliminates D_m retrieval ambiguity. Unlike DDV, absolute V_D measurements are affected by vertical air motions. However, the suggested V_D (35 GHz) threshold value is relatively high and typical air motions in widespread stratiformlike precipitation are generally within a few tenths of 1 m s^{-1} (e.g., Giangrande et al. 2012). Therefore, these motions are not expected to significantly affect thresholding.

Comparisons of Figs. 1a and 1b reveal that the data scatter for JWD and Parsivel datasets differ somewhat for larger drop populations (i.e., red dots in figures). This may be explained in part by different sampling efficiencies of these two disdrometer types. This issue, however, is

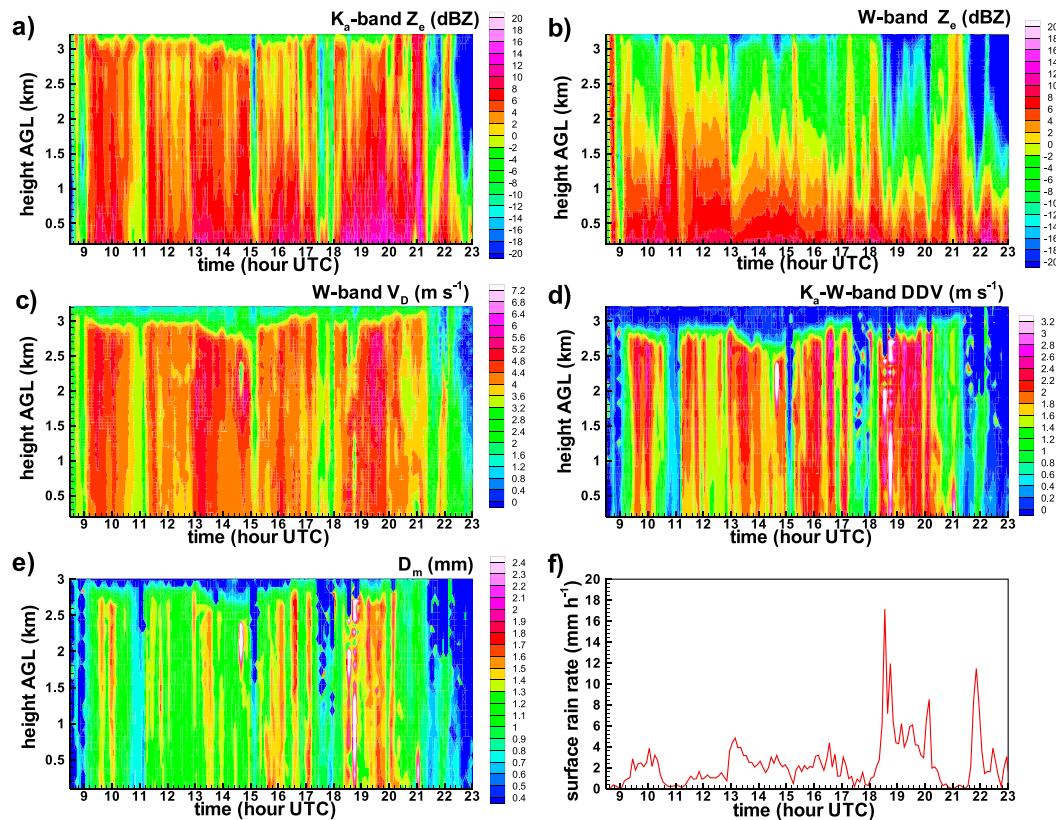


FIG. 2. Vertically pointing precipitation mode measurements of (a) MMCR- and (b) WACR-equivalent reflectivity factors, (c) WACR Doppler velocities, and (d) Ka-W-band DDV during the rainfall event on 1 May 2007. The D_m retrievals and surface rain-rate JWD estimates are shown in (e) and (f), respectively.

not expected to significantly affect the retrievals when thresholding, which was described above, is implemented.

The overall data scatter relative to the fit curve for D_m between 0.5 and 2.0 mm can be characterized by the normalized mean absolute difference (NMAD),

$$NMAD = \langle |D_{m1} - D_{m2}| \rangle / \langle D_{m1} \rangle 100\%, \quad (4)$$

where D_{m1} and D_{m2} are D_m values from the disdrometer data and the fit [Eqs. (3)], respectively (for a given DDV), and angular brackets mean averaging. The NMAD for 25 628 data points from the two DSD datasets (Figs. 1a and 1b) is about 18%. For the purpose of illustration, Figs. 1c and 1d show scatterplots of D_m and DDV for S-W-band and S-Ka-band frequency pairs, respectively.

3. Applications of the Ka-W-band DDV approach to estimate characteristic drop size

The ARM Program began occasional collocated Ka-W-band radar observations during spring 2007, when the W-band ARM Cloud Radar (WACR) was

deployed near the vertically pointing 35-GHz millimeter-wavelength cloud radar (MMCR) at the Southern Great Plains (SGP) facility [see Giangrande et al. (2012) for details on these radars]. Figure 2 shows time-height cross sections of radar measurements on a common grid and D_m retrievals using Eqs. (3) for a ~ 14 -h precipitation event on 1 May 2007. Prior to retrievals, observed Doppler velocities were corrected for air density changes with height according to Foote and du Toit (1969).

Except for some regions aloft (i.e., white areas), retrieved D_m values in Fig. 2e are generally less than about 2 mm and correspond to Ka-band $V_D < 6.5 m s^{-1}$. Figure 3 shows comparisons of DDV-based D_m retrievals at the lowest radar height (~ 0.1 km) with estimates from a ground-based JWD collocated with the radars. These estimates are used as a proxy for the “ground truth.” To minimize the influence of sample volumes and advection, comparisons are given for 6-min averages. Overall, the time series of radar and disdrometer-derived D_m values follow each other rather well in the entire range of observed drop sizes. The corresponding correlation coefficient is 0.88.

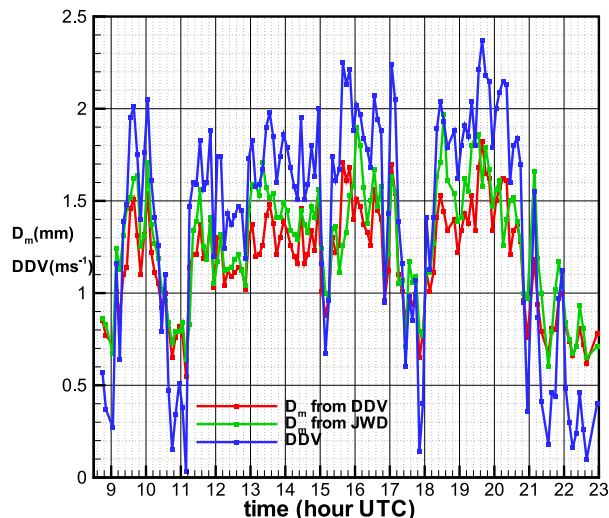


FIG. 3. MOCR–WACR DDV measurements for the SGP rain event on 1 May 2007 at the lowest height above the ground, and the corresponding retrievals (corrected for the air density dependence of Doppler velocity) and disdrometer estimates of D_m .

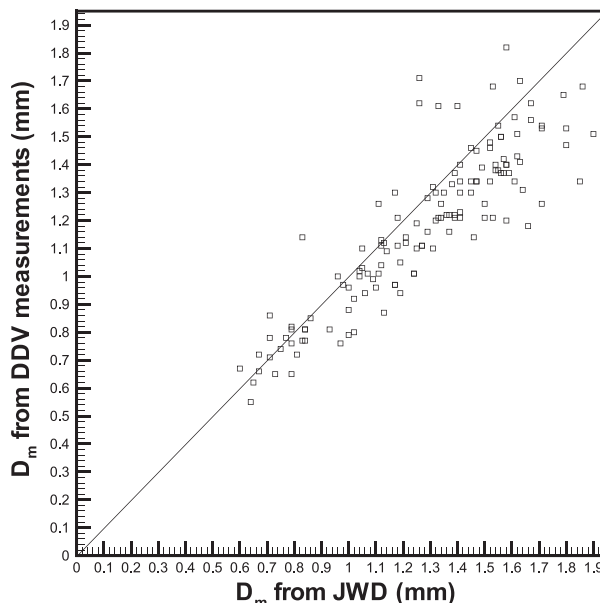


FIG. 4. A scatterplot between DDV-based retrievals and ground-based estimates of D_m for the event shown in Fig. 3.

The comparisons are shown as a scatterplot in Fig. 4. The near-ground D_m values from Ka–W-band DDV measurements cover the entire unambiguous retrieval interval of drop characteristic sizes. The radar-derived values are biased low by $\sim 9\%$ relative to the JWD estimates, and the corresponding mean differences expressed in the NMAD are around 14%, which is within the expected retrieval error. The overall agreement between DDV-based and ground truth D_m values is encouraging given the fact that Eqs. (3), used here for retrievals, were derived from large datasets collected independently without accounting for any case-specific information. For illustration, the 1 May 2007 DDV-based D_m data as derived from the SGP disdrometer are also shown in Fig. 1b. While being in the general scatter area, these data suggest some higher D_m values (for a given DDV) than predicted by the fits [Eqs. (3)]. This explains, in part, a small bias in Fig. 4.

DDV-based D_m retrieval errors are mainly coming from two major sources: the D_m –DDV correspondence uncertainty [i.e., Eq. (3) uncertainty] and DDV measurement errors. The former uncertainty source is characterized by the overall data scatter around the fits [Eqs. (3)]. As shown previously, this data scatter for the approximate interval of unambiguous D_m retrievals between about 0.5 and 2.0 mm is, on average, around 18%.

Figure 5 shows DDV measurements between about 2230 and 2300 UTC (1 May 2007) in drizzlelike precipitation at higher radar gates (Figs. 2a–d) where

Rayleigh scattering is expected for both frequencies. The mean DDV for this data subset is around 0 m s^{-1} as expected, and the standard deviation is 0.09 m s^{-1} . It can be suggested that this standard deviation value is representative of the DDV measurement error. Propagating this DDV error through Eqs. (3) results in $\sim 10\%$ D_m average retrieval uncertainty in the retrievable range of mean mass-weighted drop sizes. Assuming that the two error sources mentioned above are independent, the total D_m retrieval uncertainty

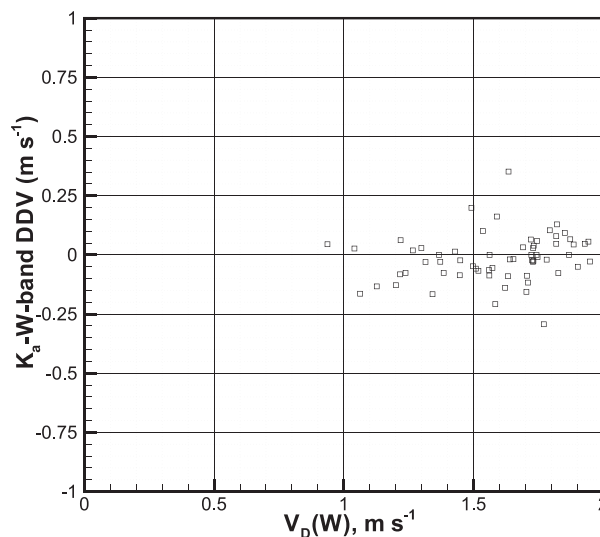


FIG. 5. Ka–W-band DDV and W-band vertical Doppler velocity scatterplot in drizzlelike precipitation.

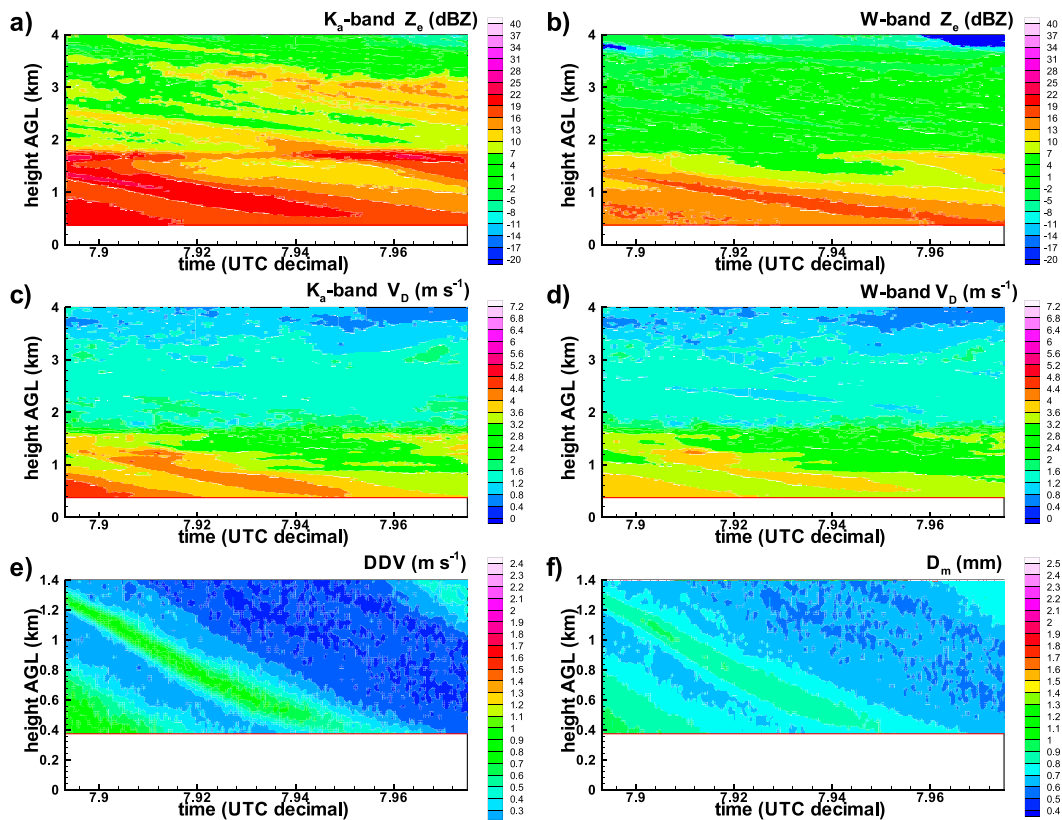


FIG. 6. Vertically pointing mode measurements of (a),(c) Ka-band-equivalent and (b),(d) W-band-equivalent (a),(b) reflectivity factors, (c),(d) Doppler velocities, and (e) Ka–W-band DDV during the rainfall event on 21 Jun 2016 at the Oliktok Point ARM facility. (f) Corresponding D_m retrievals.

from Ka–W-band DDV measurements can be estimated as a square root of the sum of squares of errors due to the two aforementioned error contributions. Such an estimate of the mean total uncertainty provides values of about 21%.

Another illustration of the approach is shown in Fig. 6. The measurements were taken with a new version of the ARM dual-wavelength scanning cloud radar, which was deployed at the Oliktok Point mobile facility (71.495°N, 149.866°W). The Ka- and W-band radar channels share a common pedestal and have similar beam widths ($\sim 0.33^\circ$). Measurements at both wavelengths are closely matched in space and time. A 30-min cycle baseline scanning procedure includes a 5-min period of vertically pointing. One such period during a 21 June 2016 rain event is shown in Fig. 6. The gate spacing of radar measurements along the beam is 15 m, and the temporal resolution of Doppler moment measurements is 2 s.

The melting layer of this stratiform event is seen at an altitude of about 1.6–1.8 km (Fig. 6). The observed Ka-band vertical Doppler velocity values are within the threshold of $6.9 m s^{-1}$, which allows for unambiguous

retrievals of mean mass-weighted raindrop sizes D_m . The corresponding retrievals (Fig. 6f) were performed for a layer between 0.375 km (i.e., the lowest radar range gate) and 1.4 km to minimize the influence of partially melted hydrometeors. The surface-based disdrometer measurements were not available for this event.

4. Conclusions

Collocated dual-frequency (Ka and W bands) radar measurements of the difference in mean vertical Doppler velocities can be used for retrievals of characteristic raindrop sizes, such as mean mass-weighted diameters D_m . A DDV– D_m relation is derived based on a large number of observed DSDs. Unambiguous retrievals of D_m are available in the approximate drop diameter interval between 0.5 and 2.0 mm if a Ka-band based Doppler velocity threshold of about $6.9 m s^{-1}$ (as referenced to the normal atmospheric conditions) is used to identify potentially ambiguous retrievals. The expected combined retrieval uncertainties due to DSD shape variability and DDV measurement errors are, on average, about 21%.

Unlike the retrievals based on reflectivity dual-frequency ratios (e.g., Matrosov 1993, 2011), DDV-based retrievals of hydrometeor characteristic sizes are immune to radar calibration errors and differential attenuation effects. Compared to Doppler spectrum-based methods, these retrievals are expected to be less susceptible to Doppler spectrum broadening. Vertical air motions do not affect DDV-based retrievals. Future intercomparisons of the DDV-based retrievals with estimates from the dual-frequency radar Doppler spectral techniques will be useful for better understanding the advantages and limitations of different approaches. In the future, estimates of characteristic drop sizes available from DDV measurements can be used to constrain relations between rain water content (RWC) and non-attenuated reflectivity in a manner suggested by Atlas et al. (1995) for inferring ice water content in ice clouds. Measurements of nonattenuated Rayleigh reflectivities for RWC retrievals, which are coincident with cloud radar data at the ARM facilities, can come from calibrated data of 915-MHz profilers.

A case study using the ARM MMCR and WACR measurements during a predominantly stratiform 14-h rain event indicated general robustness of the Ka–W DDV method for characteristic drop size retrievals in the unambiguous retrieval range. Comparisons of DDV-based retrievals of D_m at the lowest height with independent estimates of this parameter from surface disdrometer measurements indicated good agreement. New ARM Ka–W-band dual-wavelength cloud radars present a convenient tool for DSD parameter retrievals.

Acknowledgments. This work was supported by the U.S. Department of Energy's Atmospheric Systems Research Program under Award DE-SC0013306. ARM data are available from www.archive.arm.gov. Discussions with G. de Boer and C. Williams are acknowledged.

REFERENCES

- Adirosi, E., L. Baldini, F. Lombardo, F. Russo, F. Napolitano, E. Volpi, and A. Tokay, 2015: Comparison of different fittings of drop spectra for rainfall retrievals. *Adv. Water Resour.*, **83**, 55–67, doi:10.1016/j.advwatres.2015.05.009.
- Atlas, D., S. Y. Matrosov, A. J. Heymsfield, M. D. Chao, and D. B. Wolff, 1995: Radar and radiation properties of ice clouds. *J. Appl. Meteor.*, **34**, 2329–2345, doi:10.1175/1520-0450(1995)034<2329:RARPOI>2.0.CO;2.
- Brandes, E. A., G. Zhang, and J. Vivekanandan, 2005: Corrigendum. *J. Appl. Meteor.*, **44**, 186, doi:10.1175/1520-0450(2005)44<186:C>2.0.CO;2.
- Bringi, V. N., and V. Chandrasekar, 2001: *Polarimetric Doppler Weather Radar: Principles and Applications*. Cambridge University Press, 636 pp.
- Ekerete, K.-M. E., F. H. Hunt, J. L. Jeffery, and I. E. Otung, 2015: Modeling rainfall drop size distribution in southern England using a Gaussian Mixture Model. *Radio Sci.*, **50**, doi:10.1002/2015RS005674.
- Foote, G. B., and P. S. du Toit, 1969: Terminal velocity of raindrops aloft. *J. Appl. Meteor.*, **8**, 249–253, doi:10.1175/1520-0450(1969)008<0249:TVORA>2.0.CO;2.
- Giangrande, S. E., E. P. Luke, and P. Kollias, 2012: Characterization of vertical velocity and drop size distribution parameters in widespread precipitation at ARM facilities. *J. Appl. Meteor. Climatol.*, **51**, 380–391, doi:10.1175/JAMC-D-10-05000.1.
- Joss, J., and A. Waldvogel, 1967: Ein Spektograph für Niederschlagsstropfen mit automatischer Auswertung. *Pure Appl. Geophys.*, **68**, 240–246, doi:10.1007/BF00874898.
- Liao, L., R. Meneghini, L. Tian, and G. M. Heymsfield, 2008: Retrieval of snow and rain from combined X- and W-band airborne radar measurements. *IEEE Trans. Geosci. Remote Sens.*, **46**, 1514–1524, doi:10.1109/TGRS.2008.916079.
- Löffler-Mang, M., and J. Joss, 2000: An optical disdrometer for measuring size and velocity of hydrometeors. *J. Atmos. Oceanic Technol.*, **17**, 130–139, doi:10.1175/1520-0426(2000)017<0130:AODFMS>2.0.CO;2.
- Matrosov, S. Y., 1993: Possibilities of cirrus particle sizing from dual-frequency radar measurements. *J. Geophys. Res.*, **98**, 20 675–20 683, doi:10.1029/93JD02335.
- , 2010: Evaluating polarimetric X-band radar rainfall estimators during HMT. *J. Atmos. Oceanic Technol.*, **27**, 122–134, doi:10.1175/2009JTECHA1318.1.
- , 2011: Feasibility of using radar differential Doppler velocity and dual-frequency ratio for sizing particles in thick ice clouds. *J. Geophys. Res.*, **116**, D17202, doi:10.1029/2011JD015857.
- , R. Cifelli, P. J. Neiman, and A. White, 2016: Radar rain-rate estimators and their variability due to rainfall type: An assessment based on Hydrometeorology Testbed data from the southeastern United States. *J. Appl. Meteor. Climatol.*, **55**, 1345–1358, doi:10.1175/JAMC-D-15-0284.1.
- Sheppard, B. E., and P. I. Joe, 1994: Comparisons of raindrop size distribution measurements by a Joss–Waldvogel disdrometer, a PMS 2DG spectrometer, and a POSS Doppler radar. *J. Atmos. Oceanic Technol.*, **11**, 874–887, doi:10.1175/1520-0426(1994)011<0874:CORSDM>2.0.CO;2.
- Tian, L., G. M. Heymsfield, L. Li, and R. C. Srivastava, 2007: Properties of light stratiform rain derived from 10- and 94 GHz airborne Doppler radar measurements. *J. Geophys. Res.*, **112**, D11211, doi:10.1029/2006JD008144.
- Tridon, F., and A. Battaglia, 2015: Dual-frequency radar Doppler spectral retrieval of rain drop size distributions and entangled dynamics variables. *J. Geophys. Res. Atmos.*, **120**, 5585–5601, doi:10.1002/2014JD023023.
- Williams, C. R., R. M. Beauchamp, and V. Chandrasekar, 2016: Vertical air motions and raindrop size distributions estimated from mean Doppler velocity difference from 3- and 35-GHz vertically pointing radars. *IEEE Trans. Geosci. Remote Sens.*, **54**, 6048–6060, doi:10.1109/TGRS.2016.2580526.
- Wobus, H. B., F. W. Murray, and L. R. Koenig, 1971: Calculations of the terminal velocity of water drops. *J. Appl. Meteor.*, **10**, 751–754, doi:10.1175/1520-0450(1971)010<0751:COTTVO>2.0.CO;2.